

# Observations of a tornadic supercell over Oxfordshire using a pair of Doppler radars

Chris Westbrook<sup>1</sup> and Matt Clark<sup>2</sup>

<sup>1</sup> Department of Meteorology, University of Reading, Reading, UK

<sup>2</sup> Met Office, Exeter, UK.

## Introduction

On 7 May 2012 between approximately 1500-1600 UTC (4-5pm BST) a small tornado was reported by a number of observers in Witney, Kidlington and Bicester in Oxfordshire (see White 2012; Jones 2012; many more details and photographs/videos can be found by searching the world wide web). The strong winds associated with this tornado led to damage of trees, roofs and streetlights. Damage site investigations, conducted by members of the Tornado and Storm Research Organisation (TORRO: [www.torro.org.uk](http://www.torro.org.uk)), subsequently revealed a 17km-long track of intermittent damage to the north and west of Oxford (S. P. Culling, personal communication, 2012). In addition to the strong winds in the tornado itself, heavy precipitation and reasonably large hailstones ( $\approx 1$ -1.5cm diameter) were also reported. Thunder and lightning were also associated with this storm, and lightning strike locations, as detected by the Met Office Arrival Time Difference Network (figure 1), clearly show its progression throughout the afternoon as it tracked over the Cotswolds and Oxfordshire, and on into the home counties.

There have been few previous detailed observations of thunderstorms associated with tornadoes in the UK, and we are only aware of a handful of cases which have been probed using Doppler radar (Chapman et al 1998, Clark 2011, 2012). In particular, we are interested to determine whether the Oxfordshire tornado was associated with the presence of a 'supercell' - a long-lived, rotating thunderstorm, which often produces large volumes of precipitation including hail, lightning and strong surface winds over timescales significantly longer than the lifetime of a normal convective cell (Browning and Ludlam 1962; Moller *et al.*, 1994).

In this letter, we report observations of the dynamics and precipitation structure of the Oxfordshire storm over its lifetime, by making use of two Doppler radars, which

operate continuously as part the Met Office radar network. More details of the network and an overview of the basic principles of weather radar may be found in the Met Office's Fact Sheet number 15 (UK Met Office, 2009) and in a recent issue of *Weather* (Kitchen and Illingworth 2011). The radars perform a series of scans at 5 different elevation angles between 1-9°, repeated every 5 minutes. This regular sequence allows us to track the temporal evolution of the storm, and to obtain some information about its vertical structure. Although the resolution of the radar data ( $\approx 0.3 \times 1 \times 1$ km at the range of the storm in this case) is far too coarse to observe the tornado itself (which is typically  $< 0.1$ km wide), it does offer a valuable means to study the structure of the storm which produced it.

## Surface observations and analysis

Surface station measurements of pressure and temperature indicate that the storm analysed here formed in the vicinity of a warm front associated with a mesolow (a mesoscale low pressure feature). Figure 2a shows the situation at 1400 UTC. The mesolow is centred near Bristol, with a central pressure of  $\approx 1008$ mb. By 1500 UTC (figure 2b) the mesolow had tracked northeast and was centred near Swindon. A cold front extended southwest from the mesolow, and the radar composite (not shown) reveals a line of showers running along it. Meanwhile, a swath of warm air with SSW'ly surface winds is present over much of southern England, with a warm front at the northern edge of this airmass, extending across Gloucestershire and Oxfordshire. Along or just north of the front itself, two heavily precipitating storms were observed to form. The first, marked as a green dot in figure 2a,b, is the long-lived thunderstorm which will be the focus of this paper, and is associated with the long track of lightning strokes in figure 1 (marked 'Oxfordshire storm'). The second ('storm #2') was much shorter-lived, but this storm also produced intense precipitation and frequent lightning (see short track

of strokes in figure 1) during its lifetime, albeit with no tornado reports.

The formation of tornadoes within storms occurring along or just on the cool side of warm fronts (or other air mass boundaries) has been observed on numerous occasions in the USA. Such events have also previously occurred in the UK. A well-known recent example is the Birmingham tornado of 28 July 2005 (Smart, 2008; Groenemeijer *et al.*, 2011). Tornado development is especially favoured in such cases by the large changes in wind direction and speed with height in the vicinity of the frontal boundary, and resulting large values of low-level storm-relative helicity (a measure of potential updraught rotation). Of possible significance in the present case is that the northward component of motion of the warm front and the storm was approximately the same, so that the storm remained in a similar location, relative to the front, for several hours (cf. figures 2a and b).

### Track of the Oxfordshire storm

To give the reader an overview of the storm's motion we have derived its track from the radar scans. Because this thunderstorm was relatively isolated, and more intense than others present over southern England at this time, we were able to simply identify the pixel of heaviest precipitation in each scan (from the lowest beam elevation, every 5 minutes), and tracked that location between 1400 and 1700 UTC as the storm moved northeast over Wiltshire, Gloucestershire and Oxfordshire. The track is shown in figure 2: overlaid on this image are the locations at which tornados were reported, and these are collocated with the track of the storm. Note also the match with the track of the lightning location reports in figure 1 (note the different map projections used however). The location of the radar used for the tracking (Chenies in Hertfordshire) is shown in red on figures 1 and 3.

The speed and direction of the storm was approximately constant over the period shown here, at 9.5m/s from a bearing of 238°. Analysis of the motion of other showers present on the same afternoon reveals that the thunderstorm analysed in this paper moved  $\approx 15^\circ$  to the right relative to the other rain cells; this movement to the right of the winds is often a characteristic of supercell storms (Browning 1964).

The evolution of the maximum radar reflectivity measured in the storm as a function of time is shown in figure 4. There is a marked increase in precipitation intensity between 1400 and 1445 UTC, rising from  $\approx 47$ dBZ at 1400 to 62dBZ at 1445. As a guide, for raindrops alone 47dBZ corresponds to a rainrate of 32mm/hr, whilst 62dBZ

corresponds to 270mm/hr (Rogers 1979)<sup>1</sup>. In practice the presence of reflectivity values in excess of 55dBZ are usually considered a strong indicator that there are large (1cm diameter or larger), wet hailstones present (see, for example, Auer 1972), which are extremely reflective to radar because of their large size relative to raindrops – and as noted earlier, marble-sized hailstones were indeed reported at the surface in association with the storm.

From 1445-1745 UTC the peak reflectivity was relatively steady, decreasing slightly from 63dBZ at 1500 to 58dBZ at 1745. This quasi-steady-state production of heavy precipitation and hail for 3 hours is a further indication that the storm was likely a supercell, rather than an ordinary thunderstorm cell, which typically has a lifetime of only 30 minutes or so.

After 1745 UTC the storm tracked into Hertfordshire and Bedfordshire and rapidly decayed over the next 15 minutes, with peak reflectivities falling to a mere 32dBZ (equivalent to 4mm/hr of rain) by 1800 UTC<sup>2</sup>.

### Precipitation structure

Figure 5 shows a sequence of radar reflectivity snapshots between 1500 and 1600 UTC, corresponding to the period of peak precipitation and tornado occurrence. We have used data from the lowest elevation angle ( $1^\circ$ ) - note that because of the storm's distance from the radar, the radar

---

<sup>1</sup> Absolute calibration of weather radars is difficult, and the Met Office radar rainfall data is normally adjusted operationally by a complex algorithm (Harrison et al 2000) in order to match radar-retrieved rainfall rates to surface raingauge observations. For the analysis here, we wish to utilise the radar reflectivity data itself, and a different method is required. The measurements were therefore calibrated by intercomparison with the *CAMRa* dual-polarisation weather radar at the Chilbolton Observatory (Goddard et al 1994a), during light and moderate rainfall on a showery day during April 2012. Since the Chilbolton radar has been absolutely calibrated using the technique described by Goddard et al (1994b), this allows us to infer a calibration factor for the Met Office radars. We estimate a  $\pm 2$ dB uncertainty associated with the comparison and adjustment of the Met Office reflectivity data, in addition to the  $\pm 0.5$ dB uncertainty inherent in the Goddard technique.

<sup>2</sup> We note that after 1700 UTC a number of other intense storms moved into range of the Chenies radar and it became necessary to track the storm manually rather than by the simple algorithm above - the grey triangles in figure 3 are estimated peak values from this manual tracking.

beam is approximately 1.2km above the surface where it intersects the storm. The precipitation pattern is characterised by a curved region of heavy precipitation at the southern tip of the storm: this 'hook echo', most clearly seen in the 1530 UTC snapshot, is a characteristic feature of supercells (Browning 1964) and is associated with the cyclonic rotation present in such storms. Furthermore, Forbes (1981) found that 84% of storms exhibiting hook-echoes were tornadic. There is a suggestion in figs 5a-c that the hook feature progressively 'wraps-up' cyclonically over the course of these three snapshots. Tornadoes have been observed to occur during this wrap-up phase in some previously studied cases (e.g. Doswell and Lemon 1990), and we note that in fig 5c (1600UTC) that Bicester lies directly at the centre of this wrap-up region.

Since a number of scans are performed at higher elevations, we may also infer something of the 3D structure of the storm. Figure 6 shows a visualisation of this 3D structure for 1530 UTC, constructed from scans at 1.2, 2.2, 4.3 and 6.2km height (relative to the radar antenna itself which is sited  $\approx$ 150m above mean sea level). Here we show contours corresponding to the probable location of large hail (taken as the region enclosed by the 60dBZ contour, in purple), heavy rain (45dBZ, in yellow) and a broader envelope of weaker precipitation (30dBZ in blue-grey) – these colours match the colour scales in figure 4. Note the sloped region of precipitation (blue-grey contour) overhanging the precipitation-free region which the hook echo curls around at low levels. The latter region was identified by Browning (1964) who referred to it as a 'vault'. The vault is associated with a strong updraught, in which there has not yet been time during the ascent to produce precipitation particles large enough to be detected by the radar.

From the viewpoint shown in figure 6, the region of hail (purple contours) forms a curved, elongated structure. There is some suggestion of a domed top above this region, formed as the updraught overshoots the level at which parcels become negatively buoyant; however the rather coarse vertical sampling of the radar makes this difficult to identify definitively. More easily observed is the downward slope in the uppermost contour of the light and heavy precipitation areas (blue-grey and yellow in figure) as one moves downwind (northeast) from the updraught centre, showing that precipitation extended to the greatest height close to the updraught itself. These structures are consistent with those observed in supercells elsewhere (e.g. Doswell and Lemon 1990).

Of note is that the storm observed here is significantly shallower than the 'classic' supercell, as described by Browning and Ludlam (1962). Whereas their storm was  $\approx$

12km deep, our storm by comparison has no echoes  $>$ 25dBZ in the cross-section at 6.2km; indeed only a few pixels of weak echoes (15-20dBZ, close to the limit of detectability at this range), located directly above the updraught, were detected at this height (these are likely part of the dome structure noted above). Unfortunately there were no soundings in the vicinity of the storm to provide data on the thermodynamic stability of the atmosphere at the time of storm occurrence. However, vertical profiles of the Met Office operational 1.5km numerical weather prediction model for the grid box corresponding to Chilbolton Observatory in Hampshire ( $\approx$ 75km to the south of the storm itself, within the warm sector) are routinely archived and hence readily available for analysis. This forecast did correctly capture the swath of warm air over southern England and predicted the outbreak of heavy showers along the warm front, suggesting that the model should provide a reasonable representation of the thermodynamic profile of the atmosphere at that time. Figure 7 shows the profile for 1600 UTC as a skew-T-log-P diagram. Much of the troposphere has a lapse rate close to that of well-mixed saturated air, whilst at altitudes  $>$ 9km the air in the stratosphere is quasi-isothermal and very dry. From 6-9km there is a layer of dry air that has a very shallow lapse rate and hence is very stable. This feature could indicate the presence of a tropopause fold; regardless, this thermodynamic structure was present in profiles over Chilbolton for at least 4 hours. Furthermore, a similar layer of dry, stable air was present in the Camborne and Watnall 1200 UTC radiosonde ascents (not shown). It therefore seems likely that this apparently widespread layer of stable air was responsible for the relatively limited depth of the Oxfordshire storm.

#### **Dynamical structure: dual-doppler wind measurements**

With a Doppler radar, it is possible to measure the radial component of the velocity of the raindrops or ice crystals as they are advected towards or away from the radar. Since the observations here are all made at low elevation angles, only a few degrees above the horizontal, this is effectively the component of the horizontal wind vector resolved along the line between the storm and the radar. Figure 8 shows such radial velocity measurements at 1530 UTC from the radar at Chenies (approximately eastsoutheast of the storm at this time), and from a second radar at Deanhill in Hampshire (approximately southsouthwest of the storm at this time). Because of their relative positions (cf. figure 3), the Chenies radar samples a component which is almost perpendicular to that sampled by the Deanhill radar. The radial velocities from both radars in figure 8 can be seen to exhibit velocity 'couplets': well-defined regions of motion towards and away from the radar (relative to the overall

velocity of the storm) located in close proximity to each other, as indicated schematically by the arrows in each panel. The rapid azimuthal (i.e. in the direction normal to the radar beam) change in radial velocity over a short horizontal distance (up to 20m/s over 2km) is evidence of a likely cyclonic rotation, with vorticity  $\approx 0.02\text{s}^{-1}$ .

With a single Doppler radar (eg. Chapman et al 1998; Clark 2011,2012) a single couplet is observed. Although the presence of rotation may be inferred from such features, strictly speaking, single Doppler data only shows regions of cyclonic (or anticyclonic) shear (which may, or may not, be associated with a closed circulation), since only one component of the full horizontal wind field is observed. In our case, with two almost orthogonal sets of velocity components available, we may directly infer the presence of a cyclonically rotating air mass, as we will now show.

To estimate the full horizontal wind field in the storm, we have interpolated the Doppler velocity data from each radar onto a common grid (resolution 1.25km), and then constructed the wind vector from the two radial components at each point by recognising that each is a function of the horizontal wind speed and direction relative to the radar viewing angle, and then solving the pair of simultaneous equations which this leads to. Figure 9 shows the result of this synthesis, for three different heights (cross-sections at 1.2, 2.2, 4.3km). Here the winds are plotted as vectors (black arrows), and overlaid upon the reflectivity data (colours) for each height. On the left of the figure (panels a,b,c) we show the complete wind vector field, whilst on the right we have subtracted the large scale wind vector at 1.2km (as inferred from the region of light precipitation  $\approx 20\text{km}$  NE of the cell) to highlight the perturbations in the wind field which are associated with the storm.

Away from the immediate storm core, the wind vectors in panels a,b,c indicate a veering of the large-scale wind vector from southerly at low levels to southwesterly at 4.3km, and a strengthening of wind speed with height, consistent with the model wind profile in figure 6. However, note that along the southern flank of the heavy precipitation area, the winds are locally stronger, and noticeably rotated to the right of the large-scale flow at all heights. This is especially apparent at low levels, where it likely results from a superposition of the flow associated with the storm rotation (specifically, flow along its southern and western flanks) and the larger-scale, environmental flow.

The presence of a mesocyclone – a column of rotating air a few kilometres wide – is immediately apparent in the relative wind field in figure 9d, as indicated by the arrows

rotating anticlockwise near the hook and vault region. The rotation is also visible at 2.2km (panel e) suggesting rising air parcels tracing a (cyclonic) helical path. At 4.3km (panels c, f) there is no longer a rotation and instead the air at the top of the updraught is diverging outwards and forming an overhanging anvil above the vault.

One question of interest is the temporal continuity of this mesocyclone. Because the track of the storm was only visible to both radars at once for  $\approx 1.5$  hrs it was not possible to perform dual-doppler analyses for the storm's whole lifetime. However, well-defined couplets in the radial velocity data similar to those shown in figure 8 were observed between 1430-1730 UTC, corresponding to the period when the core reflectivity was quasi-steady (cf. figure 4). There is a suggestion in the Doppler data that rotation was also present at times before and after this period, but the couplets appear to be weaker and less well-defined.

A number of other interesting features may be identified from the slices in figure 9. A distinct V-shape is visible in the pattern of reflectivities – this is particularly clear in panel b (e.g. in the outline of the yellow contour), but also to a lesser extent in panels a and c. This feature has been dubbed the 'V-notch' and is believed to be evidence for the presence of a very strong updraught: this updraught effectively acts as an obstacle to the large scale flow, leading to two trailing wakes of precipitation downstream, forming the V-pattern in the radar echo (Klemp 1987). In addition, the overhanging region of anvil above the vault identified in figure 6 is also easily observed in these slices; e.g. by comparing the outline of the echo in the SE quadrant of the storm in panel (a) and panel (c).

## The evolution of storm #2

As noted earlier, a second, shorter-lived thunderstorm was also observed on the afternoon of 7 May 2012. Like the Oxfordshire storm this cell ('storm #2' in figure 1) was observed to track to the right of the winds and produced lightning for  $\approx 1.5$ hrs. Figure 10 shows a snapshot of reflectivity and Doppler velocity sampled by the Deanhill radar at 1500UTC, and shows the Oxfordshire cell and storm #2 side-by-side. Both have reflectivities exceeding 60dBZ indicating again the presence of large wet hailstones. Likewise, the Doppler data contain couplets of radial velocities towards and away from the radar (relative to the mean wind), indicating the presence of a mesocyclone in both storms. Storm #2's couplet was observed continuously for  $\approx 1$ hr, after which the storm rapidly decayed, at approximately 1530 UTC.

One hypothesis for the demise of this cell is that air cooled by evaporation of precipitation in the outflow of the Oxfordshire storm was ingested into the inflow region of storm #2. Another possibility is simply that there were local variations in the storm environment (for example, differences in convective available potential energy or regions of locally backed low-level winds) which favoured the Oxfordshire storm relative to its neighbour. Analysis of high resolution numerical simulations using both the Met Office unified model (H Lean and N Roberts – personal communication) and using the Weather Research and Forecasting model (D Smart – personal communication) are underway, and may provide some insight into the significance of these factors, which are not easily diagnosed from observations.

## Discussion

Our observations are consistent with the presence of a supercell. Figure 11 illustrates the key features of a supercell storm in its tornadic phase, according to Lemon and Doswell (1979). Warm moist air flows into the storm at low levels, and ascends rapidly, with air parcels tracing helical paths in the rotating updraught before flowing out at the top of the storm. Meanwhile, air entering the rear flank of the storm at upper levels is obstructed by the strong updraught. As discussed earlier, this leads to the air being forced around the updraught forming a pair of trailing wakes; however the air is forced not only around, but also downwards, flowing out along the surface forming a gust-front. Part of this gust front curls around and undercuts the inflow of warm air (as observed in figure 5) somewhat analogously to the occlusion process in a synoptic-scale cyclone. It is during this occlusion process that tornadoes often form in a supercell storm, at the interface between the warm ascending air and the cold descending air undercutting it (Markowski 2002). However, the precise mechanisms involved in tornadogenesis are still a matter of active debate and research: we refer the interested reader to Markowski's (2002) detailed review paper.

Doswell (1996) among others has emphasised that the classification of a storm as a supercell should be based not only upon the basis of the presence of reflectivity and Doppler signatures at a given point in time, but that the mesocyclone should be observed as being contiguous over a significant vertical depth, and continuous over a significant period of time. Through analysis of the Doppler radar data, we have established that both of these criteria have been met in the Oxfordshire storm: even from the crude vertical sampling used here, the mesocyclone was a minimum of 1km deep, and we observed this mesocyclone in the Doppler data continuously for at least 3 hours. We

therefore have little doubt that this storm was indeed a supercell.

The Oxfordshire storm was shallow relative to the classic supercells of Wokingham and Geary (Browning 1964). The ability of a storm only 5-6km deep to produce such intense precipitation is at first sight somewhat surprising. However, the model sounding in figure 6 may provide a clue, by telling us that the top of the storm was  $\approx -35^{\circ}\text{C}$ . This temperature is significant, because this is the temperature below which water droplets cannot remain liquid – even without the presence of any aerosols which can act as ice nuclei. Since the mechanism by which graupel, hail and raindrops grow is by collection of liquid water droplets, we suggest that a deeper storm in this case would not in fact confer any additional advantage in terms of precipitation production, because no additional liquid droplets would be available for collection.

## Conclusions

We were extremely lucky to get such a good view of the structure of the Oxfordshire supercell during its tornadic phase; as can be seen from figure 2, there is only a narrow region where the two Doppler radars at Chenies and Deanhill overlap. Moreover, the radars were at distances such that the altitude of the various cross-sections was almost the same (certainly any differences were much less than the 1km width of the radar beam), and the viewing angles were almost orthogonal to each other. These factors are key to a robust dual-Doppler analysis.

This study appears to be the first published dual-Doppler radar observations of a tornadic supercell (or indeed a tornadic storm of any kind) in the UK. Apart from being an interesting case study of a severe storm, this analysis underlines the value of the operational Doppler radar network, providing a dynamical context which can aid both the interpretation of weather events in real time, and research into storm dynamics and microphysics. This data can also be a valuable teaching tool: the analysis in this letter grew from a feature in the 'Weather and Climate Discussion' module at the University of Reading, and the Doppler radar data allowed the students to see the concepts which they had learnt about in lectures being played out in a real tornadic storm.

At the time of writing, a major upgrade of the UK radar network is underway at the Met Office, which includes the provision Doppler radar capability across the whole network. It is anticipated that this will increase the frequency with which supercells are identified and observed in the UK, and will lead to further opportunities for dual Doppler analysis of such storms in the future.

## Acknowledgements

Many thanks are due to Graeme Anderson at the Met Office who provided the lightning strike data; to Thorwald Stein at Reading for providing the code for the 3D volume plot; and to Ewan O'Connor at Reading who developed the software to convert the binary radar data into netCDF. CDW acknowledges valuable discussions with Nigel Roberts, Humphrey Lean, Sue Ballard and Rob Warren.

We thank the Met Office for making their Doppler radar data freely available, and the British Atmospheric Data Centre for distributing it. We would like to thank the staff at the SFTC Chilbolton Observatory for operation and calibration of the CAMRa radar which was used to calibrate the reflectivity data presented here.

The operational UKV numerical weather prediction model profiles used here were archived as part of the CloudNet project ([www.cloud-net.org](http://www.cloud-net.org)), and was provided by the Met Office.

## References

**Auer A** 1972: Distribution of graupel and hail with size *Mon. Wea. Rev.* **100** 325-328

**Browning KA and Ludlam FH** 1962: Airflow in convective storms *Q. J. R. Meteorol. Soc.* **88** 117-135

**Browning KA** 1964: Airflow and trajectories within severe local storms which travel to the right of the winds *J. Atmos. Sci.* **21** 634-639

**Clark MR** 2011: Doppler radar observations of mesovortices within a cool-season tornadic squall line over the UK *Atmos. Res.* **100** 749-764

**Clark MR** 2012: Doppler radar observations of non-occluding, cyclic vortex genesis within a long-lived tornadic storm over southern England *Q. J. R. Meteorol. Soc.* **138** 439-454

**Doswell CA III** 1996: What is a supercell? *Preprints, 18 th AMS Conf. Severe Local Storms (San Francisco, CA)*, Amer. Meteor. Soc., p. 641.

**Doswell CA III and Lemon LR** 1990: Severe thunderstorm detection by radar, in *Radar in Meteorology*, Ed D Atlas, American Meteorological Society, Boston, USA.

**Forbes GS** 1981: On the reliability of hook echoes as tornado indicators *Mon. Wea. Rev.* **109** 1457-1466

**Goddard JWF, Eastment JD and Thurai M** 1994a: The Chilbolton Advanced Meteorological Radar – a tool for multidisciplinary atmospheric research *Elect. & Comm. Eng. J.* **6** 77-86

**Goddard JWF, Tan J and Thurai M** 1994b: Technique for calibration of meteorological radars using differential phase *Electron. Lett.* **30** 166-167

**Groenemeijer P, Corsmeier U and Kottmeier Ch** 2011: The development of tornadic storms on the cold side of a front favoured by local enhancement of moisture and CAPE. *Atmos. Res.* **100** 765-781

**Harrison DL, Driscoll SJ and Kitchen M** 2000: Improving precipitation estimates from weather radar using quality control and correction techniques *Meteorol. Appl.* **7** 135-144

**Jones S** 2012: Tornado hits Oxfordshire as more stormy weather forecast for UK, *The Guardian* 8 May 2012, available at <http://www.guardian.co.uk/uk/2012/may/08/tornado-stormy-weather-forecast-uk>

**Klemp JB** 1987: Dynamics of tornadic thunderstorms *Ann. Rev. Fluid. Mech.* **19** 369-402

**Kitchen M and Illingworth AJ** 2011: From observations to forecasts, part 13: The UK weather radar network – past, present and future. *Weather* **66** 291-297

**Lemon LR and Doswell CA III** 1979: Severe thunderstorm evolution and mesocyclone structure as related to tornadogenesis *Mon. Wea. Rev.* **107** 1184-1197

**Markowski PM** 2002: Hook echoes and rear-flank downdrafts: a review. *Mon. Wea. Rev.* **130** 852-876

**Moller AR, Doswell CA III, Foster MP and Woodall GR** 1994: The operational recognition of supercell thunderstorm environments and storm structures. *Weather and Forecasting*, **9** 327-347

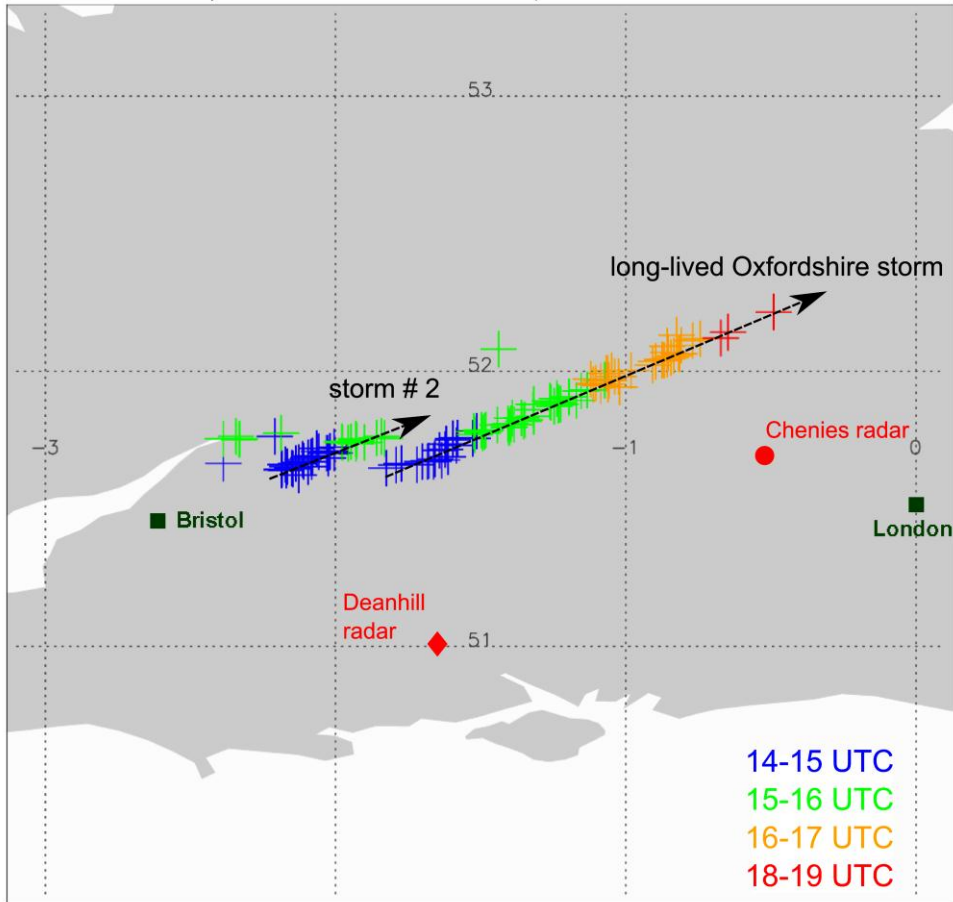
**Rogers RR** 1979: *A short course in cloud physics*. Second edition, Pergamon Press Ltd, Oxford

**Smart D** 2008: Simulation of a boundary crossing supercell – a note on the 28 July 2005 Birmingham UK event. *International Journal of Meteorology*. **33** 271-274

**UK Met Office** 2009 Fact Sheet number 15: Radar. National Meteorological Library and Archive. Available from <http://www.metoffice.gov.uk/learning/library/publications/factsheets>

**White S** 2012: The twister in Bicester: Sky turns black as tornado hits south of England, *The Mirror* 8 May 2012, available at <http://www.mirror.co.uk/news/uk-news/oxfordshire-tornado-supercell-storm-brings-823363>

ATDnet hour by hour strokes on 7th May 2012 between 14-19 UTC



© Crown Copyright 2012. Source: Met Office

Figure 1: Lightning location observations from Met Office Arrival Time Difference network. The colours indicate the period in which the lightning stroke was detected. Dashed black line is intended to guide eye, and represents the track of the storm studied in this paper.

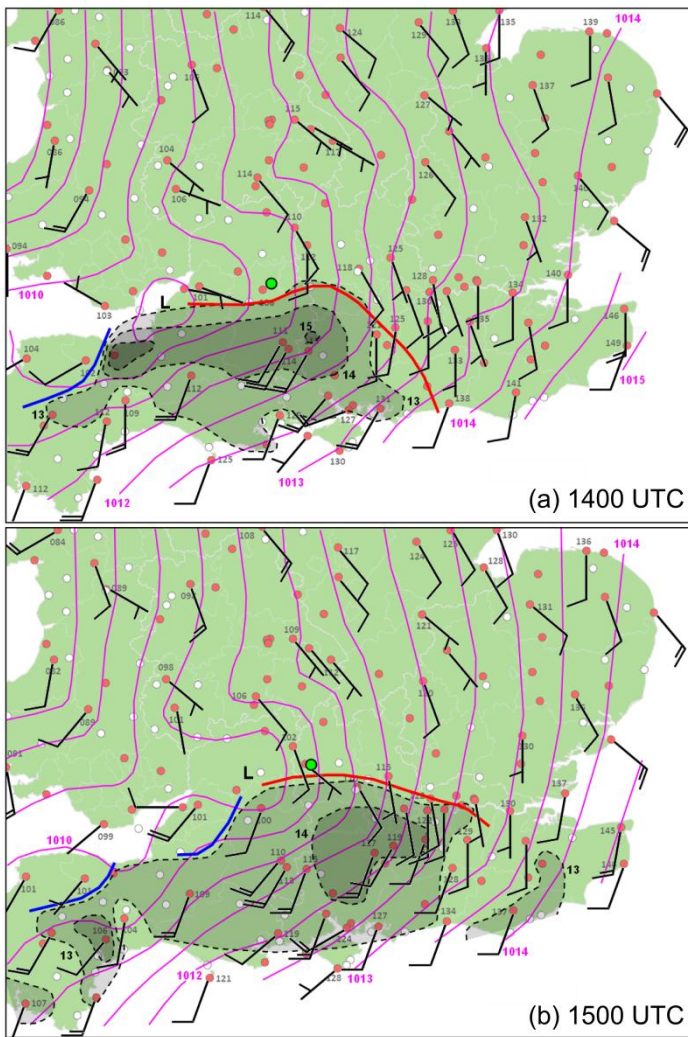


Figure 2a,b: Mesoanalyses showing surface pressure (purple contours at 0.5 hPa intervals, also shown in tenths of hPa adjacent to station circle, where measured), temperature (black dashed contours with shading; values  $\geq 13$  °C shown only), and surface winds shown as barbs using standard notation, at 1400 and 1500 UTC. Green circle indicates position of the Oxfordshire storm at that time. Red and blue bold lines indicate the analysed positions of surface warm and cold fronts, respectively.

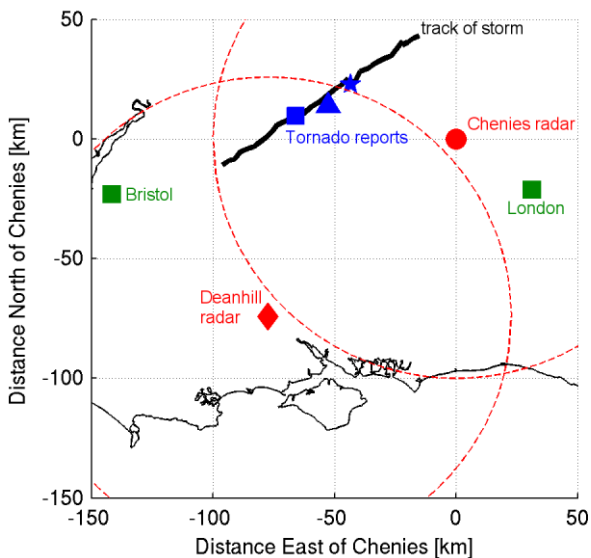


Figure 3: Path of the thunderstorm (thick black line) as it moved northeast between 1400 and 1700 UTC, derived from the position of the highest radar reflectivity in each scan. Blue symbols indicate locations where tornadoes were reported (Witney - square; Kidlington - triangle; Bicester - star). Red symbols are positions of the two radars used in this study, and the dashed red circles show the maximum range of the radars. Co-ordinates are given in distance North/East of the Chenies radar (note the differing map projection to figure 1).

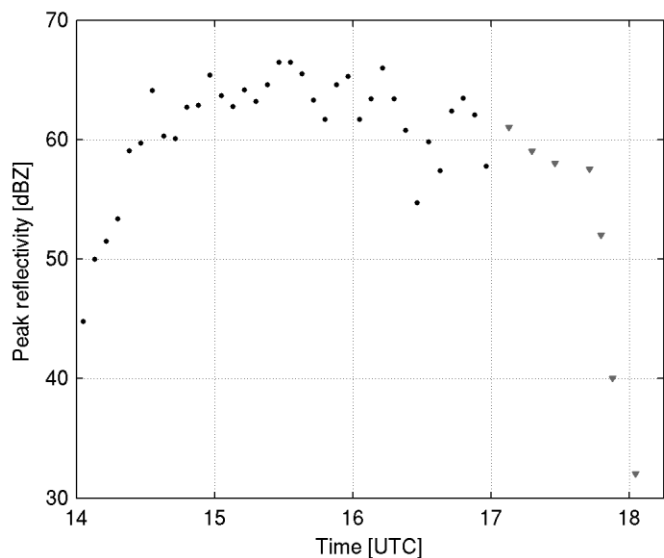


Figure 4: Evolution of the peak storm radar reflectivity as measured by the Chenies radar. Black dots are values corresponding to automatically identified storm track in figure 2. Grey triangles are manually tracked values after 1700 UTC showing eventual decay of the cell.

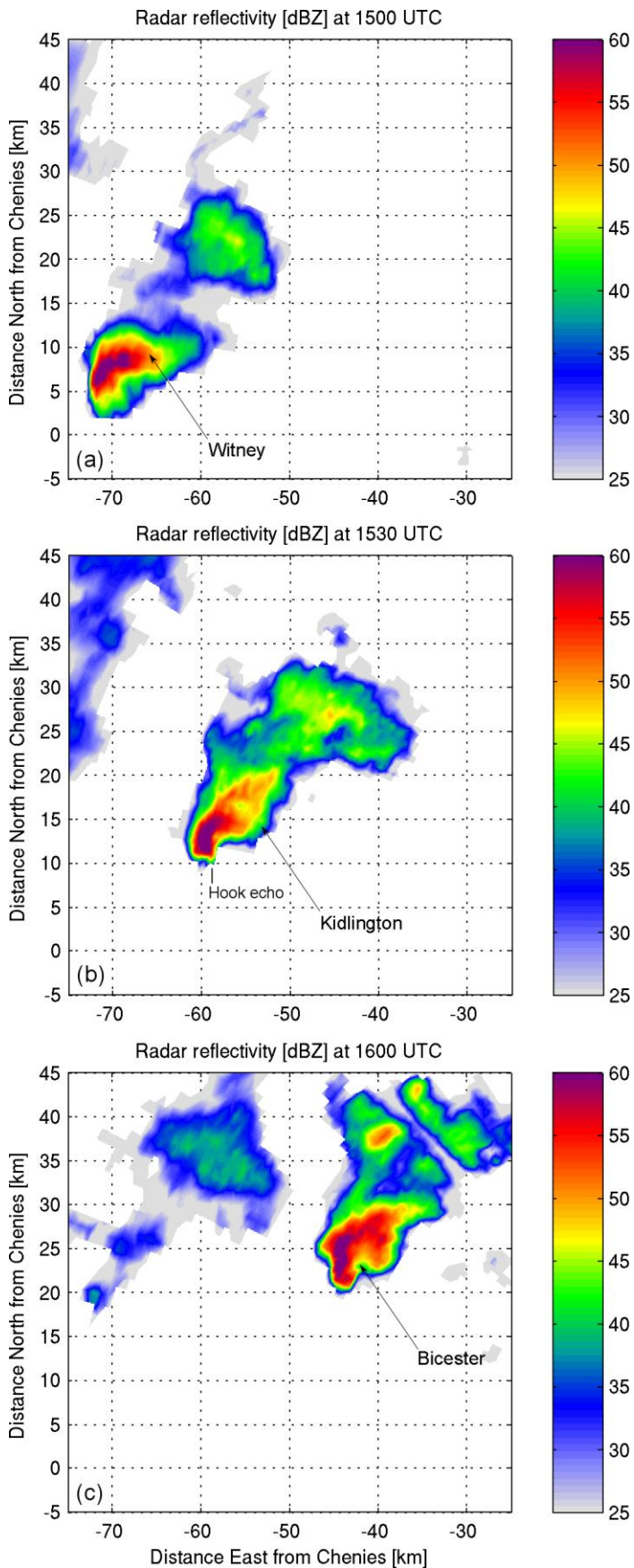


Figure 5: Sequence of snapshots of radar reflectivity at (a) 1500, (b) 1530 and (c) 1600 UTC. Note the 'hook' structure at the south-western tip of the storm (particularly visible in panel b), indicating the likely presence of a mesocyclone. The true resolution of these radar data is  $\approx 0.3 \times 1 \times 1 \text{ km}$ : here they have been interpolated onto a finer grid (100m) in order that the more subtle patterns (e.g. the hook echo) may be more easily identified by eye. The locations of Witney, Kidlington and Bicester are marked on: readers may wish to compare with the blue symbols in figure 3 for a larger-scale perspective.

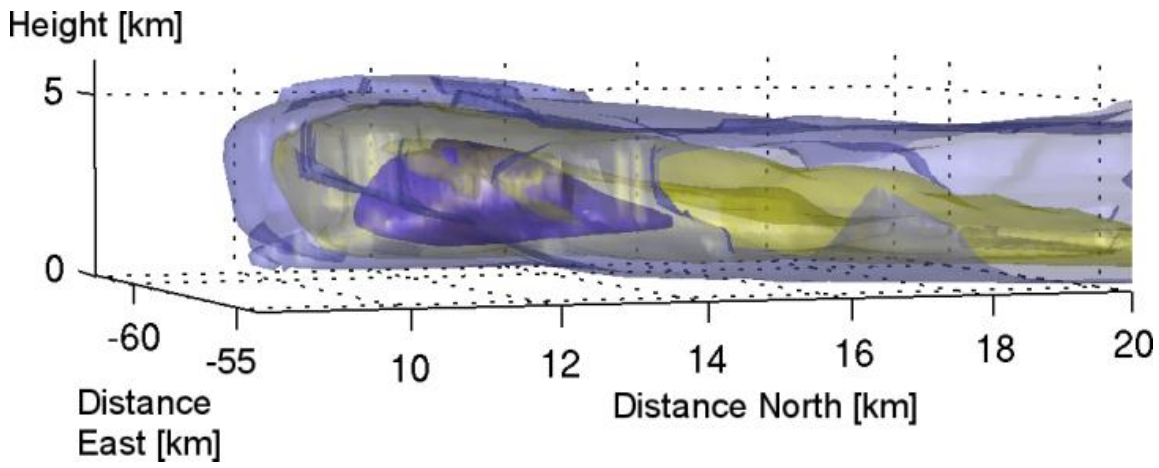


Figure 6: Three-dimensional storm structure at 1530 UTC, constructed from radar scans at four different elevations, corresponding to 1.2, 2.2, 4.3 and 6.2km height. Different colour surfaces are contours of reflectivity: blue-grey outline 30dBZ; yellow 45dBZ; purple core is 60dBZ (suggestive of the presence of large hail). Viewpoint is from east-south-east at 2.5 degrees elevation.

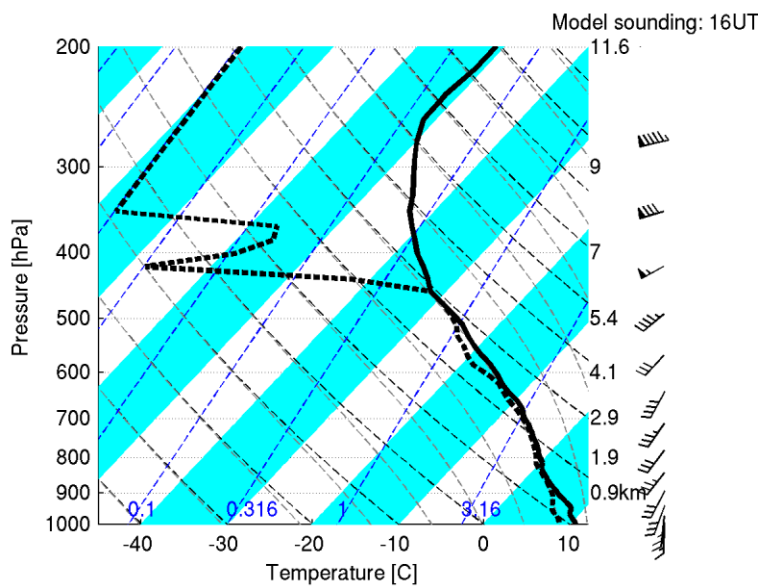


Figure 7: Skew-T-log-P diagram showing vertical profile at Chilbolton, Hampshire at 1600 UTC from UK 1.5km Met Office numerical weather prediction model.

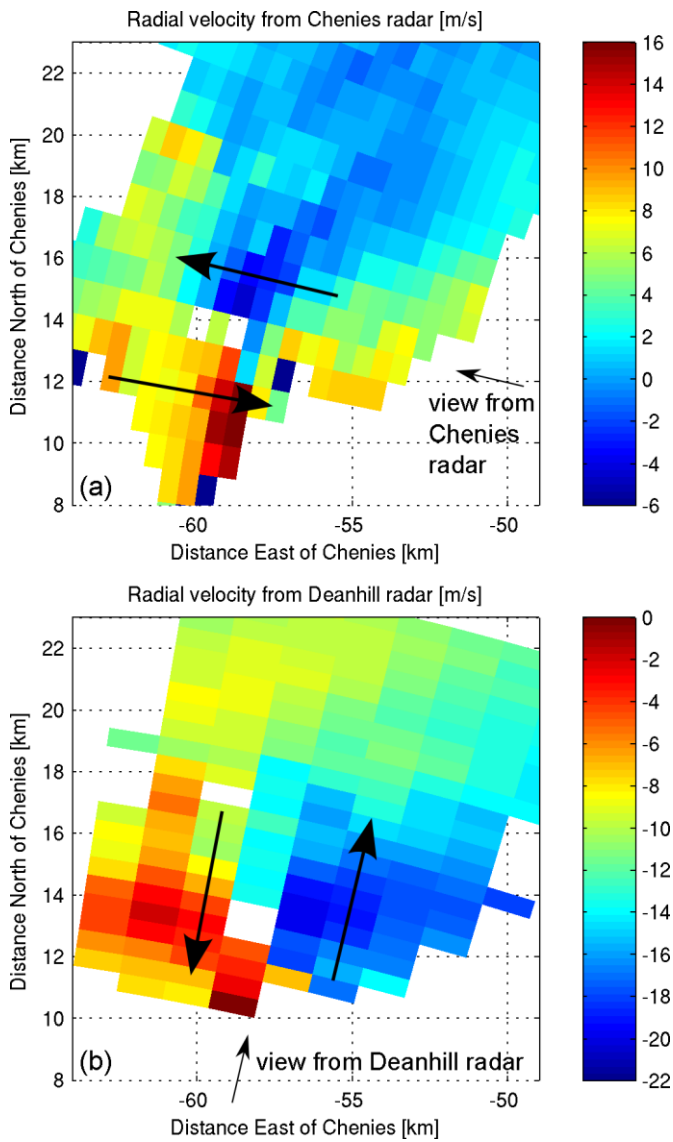


Figure 8: Radial velocities at 1530 UTC as measured by the radars at (a) Chenies and (b) Deanhill. Velocities towards the radar are positive, velocities away from the radar are negative. Small arrows indicate the viewing direction from the radar sites in each case; large arrows indicate radial components of cyclonic motion relative to the large scale flow. The data were sampled < 1 minute apart – the slightly different outline of the storm in the two panels are partly due the fact that the storm is slightly further away from the Deanhill radar and hence weak echoes at the southern-most tip of the storm are no longer detectable, and partly due to the differing geometries of the sample volumes (both 300m in range  $1^\circ$  in azimuth, but from perpendicular viewing directions).

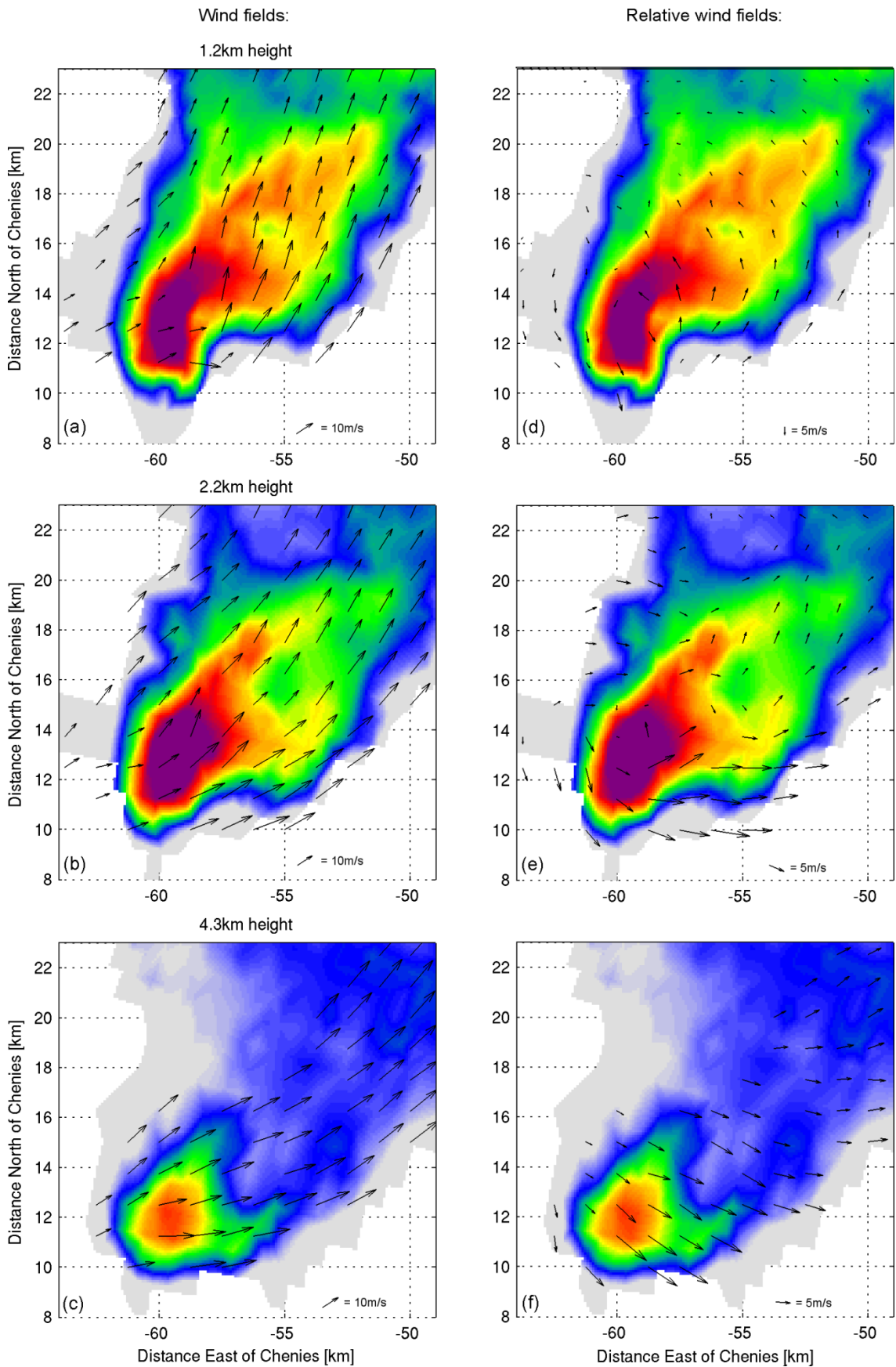


Figure 9: Dual-doppler syntheses showing the horizontal wind velocity field at 1530 UTC (arrows) overlaid on radar reflectivity data (colours – same scale as figure 4). Left hand panels: three cross-sections corresponding to different heights are shown: (a) 1.2km, (b) 2.2km, (c) 4.3km. Right hand panels (d,e,f) show the same fields, but with the large scale wind vector at 1.2km subtracted, in order to highlight the ‘storm-relative’ motions.

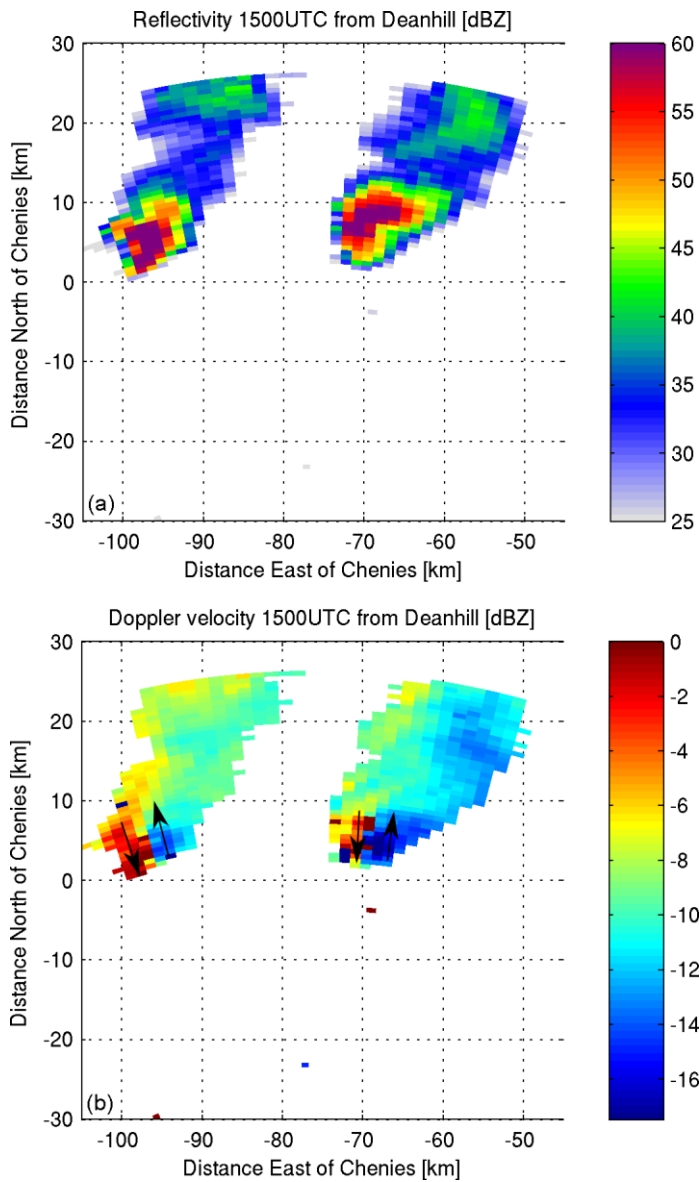


Figure 10: Snapshots of (a) radar reflectivity and (b) Doppler velocity measured by Deanhill radar at 1500 UTC. Right hand cell is the Oxfordshire storm; left hand cell is the shorter-lived 'storm #2' (see text, and figure 1). Note the couplets of radial velocity in both cases, emphasised conceptually by overlaid arrows, indicating the presence of a mesocyclone in both storms.

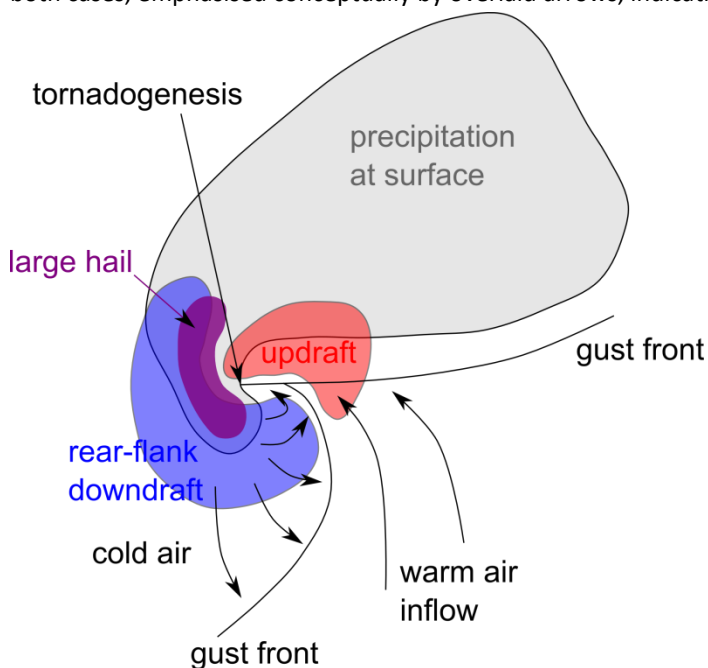


Figure 11: Schematic diagram of supercell structure – following Lemon and Doswell (1979) – compare the structure here to figs 5,9. Red areas are regions of strong ascent, blue of strong descent. Note that a region of weaker descent, not marked here, is

typically present in the weakly precipitating region at the forward-flank of the storm – see Lemon and Doswell (1979) for more details.